FLOW OF A FINE-DISPERSED HETEROGENEOUS MEDIUM IN A TURNING CHANNEL OF A GAS DUCT

A. M. Bubenchikov and A. V. Starchenko

UDC 532.529.5:532.517.4

Results of a numerical study of turbulent flow of a polydispersed two-phase mixture in a turning section of a gas duct are presented. Calculated data allow a localization of the zone of particle accumulation at the channel walls and an evaluation of efficiency of the particle entrapment in a hopper.

An up-to-date level of the development of hydrodynamics, mechanics of turbulent flows, and computing machinery offers hope for obtaining a concrete result in solving, by numerical modeling, the engineering problems involving a design of new devices in power engineering and chemical technology, as well as an improvement of their operational conditions. Numerical modeling acquires particular significance in studying flows whose reproduction in the laboratory is difficult or entirely impossible. A case in point may be aerodynamic processes occurring in boiler plants, the results of whose investigation using physical models are far from being always applicable to full-scale objects because of the so-called "scale effect." Numerical models are devoid of this shortcoming. However, they are tested and supported by the results of experimental studies, mostly performed under laboratory conditions. From this standpoint, the flows in laboratory setups, just as in the full-scale aerodynamic process, appear highly important.

The current work is concerned with modeling a polydispersed flow in a turning channel of the physical model of a boiler plant gas duct. The ultimate goal of the study is to numerically obtain the aerodynamic pattern of the flow in the turning gas-air channel in the initial geometry, to investigate the effect of a turn angle of the gas duct outlet branch on the efficiency of particle entrapment in the hopper, and to localize the zones of increased particle content in near-wall regions of the gas duct.

A mathematical model of the considered process is based on the chief postulates of the theory of interacting interpenetrating continua [1]. Polydispersity is taken into account through isolating main fractions by the function, which defines a granulometric composition of the dispersed phase. It is assumed that the particles of each phase are of spherical shape and of the same size; the density of the particle material greatly exceeds the density of the carrying medium, the volume concentration of the particles is small, and their collisions may be disregarded.

Equations defining a plane steady turbulent flow of the two-phase polyfractional medium have the form:

$$\frac{\partial}{\partial x}(\rho_i U_i) + \frac{\partial}{\partial y}(\rho_i V_i) = 0, \quad \frac{\partial}{\partial x}(\rho_i U_i U_i) + \frac{\partial}{\partial y}(\rho_i U_i V_i) =$$

$$= -\alpha_i \frac{\partial P}{\partial x} - \frac{2}{3}\frac{\partial}{\partial x}(\rho_1 K)\delta_{1i} + 2\frac{\partial}{\partial x}\left(\mu_{ti}\frac{\partial U_i}{\partial x}\right) +$$

$$+ \frac{\partial}{\partial y}\left(\mu_{ti}\frac{\partial U_i}{\partial y}\right) + \frac{\partial}{\partial y}\left(\mu_{ti}\frac{\partial V_i}{\partial x}\right) + F_{xi} - \rho_i g,$$

$$\frac{\partial}{\partial x}(\rho_i U_i V_i) + \frac{\partial}{\partial y}(\rho_i V_i V_i) = -\alpha_i \frac{\partial P}{\partial y} - \frac{2}{3}\frac{\partial}{\partial y}(\rho_1 K)\delta_{1i} +$$

$$+ \frac{\partial}{\partial x}\left(\mu_{ti}\frac{\partial V_i}{\partial x}\right) + 2\frac{\partial}{\partial y}\left(\mu_{ti}\frac{\partial V_i}{\partial y}\right) + \frac{\partial}{\partial x}\left(\mu_{ti}\frac{\partial U_i}{\partial y}\right) + F_{yi},$$

$$\frac{\partial}{\partial x}(\rho_i U_i T_i) + \frac{\partial}{\partial y}(\rho_i V_i T_i) = Q_i +$$

$$+ \frac{\partial}{\partial x}\left(\frac{\mu_{ti}}{\sigma_{hi}}\frac{\partial T_i}{\partial x}\right) + \frac{\partial}{\partial y}\left(\frac{\mu_{ti}}{\sigma_{hi}}\frac{\partial T_i}{\partial y}\right), \quad P = \rho_1^0 R T_1.$$

Scientific Research Institute of Applied Nathematics, Tomsk, Russia. Translated from Inzhenerno-Fizicheskii Zhurnal, Vol. 63, No. 1, pp. 51-57, July, 1992. Original article submitted April 30, 1991.

1062-0125/92/6301-0690$12.50 ©1993 Plenum Publishing Corporation

Dynamic and thermal interactions between the phases are determined by the following relations:

$$F_{xi}=\rho_i\frac{f_{Di}}{\tau_{pi}}(U_1-U_i),\quad F_{yi}=\rho_i\frac{f_{Di}}{\tau_{pi}}(V_1-V_i),$$

$$\tau_{pi}=\frac{\rho_p^0 d_{pi}^2}{18\mu_1};\quad f_{Di}=1+0{,}15\,\mathrm{Re}_{1i}^{0{,}687},$$

$$\mathrm{Re}_{1i}=\rho_1^0 d_{pi}\,[(U_1-U_i)^2+(V_1-V_i)^2]^{0{,}5}/\mu_1,\quad i>1,$$

$$F_{x1}=-\sum_{i=2}^{m}F_{xi},\quad F_{y1}=-\sum_{i=2}^{m}F_{yi},\quad Q_i=\frac{6\lambda_1\alpha_i\,\mathrm{Nu}_{1i}}{C_i d_{pi}^2}(T_1-T_i),$$

$$Q_1=-\Big(\sum_{i=2}^{m}Q_iC_i\Big)/C_1,\quad \mathrm{Nu}_{1i}=2+0{,}459\,\mathrm{Re}_{1i}^{0{,}55}\,\mathrm{Pr}^{0{,}33},\quad i>1,$$

where μ_1 and λ_1 are the viscosity and thermal conductivity coefficients of the carrying medium, and C_i ($i = 1, \ldots, m$) is the specific heat of unit mass of the gas or particle fraction.

Presently, the transport models which take into consideration differential equations for averaged turbulence characteristics are widely used in modeling the processes of turbulent transfer. The application of such models is indispensable in the cases when the flow is associated with separation, chemical transformations, and with the effect of a heterogeneous phase on the averaged flow and turbulent transfer processes. Such models are essentially semiempirical, however, they are appreciably more potent for taking account of the influence of physical mechanisms complicating the flow.

The current study predicts a turbulent structure of the flow from the two-equation $k-\varepsilon$ turbulence model, modified in [2] to allow for the effect of the dispersed phase on averaged turbulence characteristics:

$$\frac{\partial}{\partial x}(\rho_1U_1K)+\frac{\partial}{\partial y}(\rho_1V_1K)=\frac{\partial}{\partial x}\left(\frac{\mu_{t1}}{\sigma_K}\frac{\partial K}{\partial x}\right)+$$

$$+\frac{\partial}{\partial y}\left(\frac{\mu_{t1}}{\sigma_K}\frac{\partial K}{\partial y}\right)+\mu_{t1}G-\rho_1\varepsilon+S_K,$$

$$\frac{\partial}{\partial x}(\rho_1U_1\varepsilon)+\frac{\partial}{\partial y}(\rho_1V_1\varepsilon)=\frac{\partial}{\partial x}\left(\frac{\mu_{t1}}{\sigma_\varepsilon}\frac{\partial \varepsilon}{\partial x}\right)+$$

$$+\frac{\partial}{\partial y}\left(\frac{\mu_{t1}}{\sigma_\varepsilon}\frac{\partial \varepsilon}{\partial y}\right)+\frac{\varepsilon}{K}(c_1\mu_{t1}G-c_2\rho_1\varepsilon)+S_\varepsilon,$$

$$\mu_{t1}=c_\mu\rho_1\frac{K^2}{\varepsilon}.$$

Here $G=\left(\frac{\partial U_1}{\partial y}+\frac{\partial V_1}{\partial x}\right)^2+2\left(\frac{\partial U_1}{\partial x}\right)^2+2\left(\frac{\partial V_1}{\partial y}\right)^2$ is the dissipative function; $T_L = 5K/(12\varepsilon)$ is the local Lagrangian time scale; S_K and S_ε are the terms taking into account the particle effect on turbulence [2]:

$$S_K=-2K\sum_{i=2}^{m}\frac{\rho_i}{\tau_{pi}+T_L},$$

$$S_\varepsilon=-2\varepsilon\sum_{i=2}^{m}\frac{\rho_i}{\tau_{pi}+T_L}+2\frac{\mu_1}{\rho_1}\left(\frac{\partial K}{\partial x}\frac{\partial T_L}{\partial x}+\frac{\partial K}{\partial y}\frac{\partial T_L}{\partial y}\right)\sum_{i=2}^{m}\frac{\rho_i}{(\tau_{pi}+T_L)^2}.$$

To obtain a turbulent viscosity coefficient for the particle continuum we use the Peskin equation:

$$\frac{\mu_{ti}}{\mu_{t1}}=\frac{\rho_i}{\rho_1}\left[1-1{,}5\left(\frac{L}{H}\right)^2\frac{\Omega_i^2}{\Omega_i^2+2}\right],\quad i=\overline{2,\ m},$$

where L is the turbulence scale, $\Omega_i = 2\tau_{pi}/T_L$ is the relaxation parameter, and H is the characteristic geometric scale.

The turbulence model constants fit the standard values: $c_1 = 1.44$, $c_2 = 1.92$, $c_\mu = 0.09$, $\sigma_K = 1$, and $\sigma_\varepsilon = 1.3$.

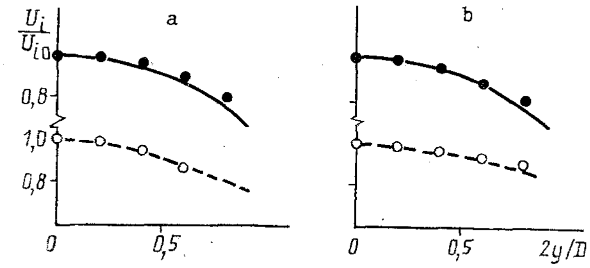

Fig. 1. Comparison of calculated results with experimental data [7] by velocity profiles of gas (solid curves) and particles (dashed curves), $d_p = 62\ \mu m$, $\rho_p = 1.2\ kg/m^3$, Re = 24,500; a) D = 0.0254 m, b) 0.0127 m.

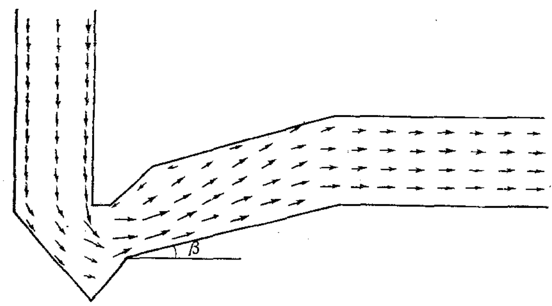

Fig. 2. Velocity field of the carrying medium.

A formulation of boundary conditions is an extremely important step of the numerical modeling. Ellipticity of the problem on calculation of a steady flow with circulation zones calls for a statement of boundary conditions on all sections of the circuit confining a flow region. Some of them are solid, and some are free boundaries, through which the liquid flow proceeeds. A solution behavior along the considered boundary section may not always be determined by one or another physical considerations. This gives rise to a need for new assumptions about properties of the derived solution.

The experience gained by now in computations of complex turbulent flows makes it possible to regard a method of wall functions, generally realized within the framework of a high Reynolds number turbulence model, as fairly well-grounded for formulating boundary conditions at the wall. According to this method, the conditions, obtained assuming that a logarithmic velocity and temperature profile is valid in the near-wall region [3], are imposed at the solid surfaces for the carrying medium. These assumptions seem quite justifiable for weakly dust-laden flows. An outlet boundary is located at a considerable distance from the zones of disturbed motion, which admits the use of mild boundary conditions for all motion characteristics:

$$\frac{\partial V_i}{\partial y} = \frac{\partial U_i}{\partial y} = \frac{\partial \rho_i}{\partial y} = \frac{\partial T_i}{\partial y} = \frac{\partial K}{\partial y} = \frac{\partial \varepsilon}{\partial y} = 0, \quad i = \overline{1, m}.$$

In studying the flows of heterogeneous media, the problem of formulating boundary conditions for the particle continuum acquires an independent meaning, the greatest complications being related to reproducing the conditions, which simulate the particle interaction with the walls. If the particles come closer to the wall at a finite velocity and elastic forces are significant, then in a certain vicinity of the wall the particle velocity (since both incident and reflected particles are present) is indeterminate. However, there are approaches which allow one to resolve this uncertainty, for example, the method [4] suggesting the introduction of a reflected particle fraction. For rather small particles it can be assumed that their velocity when approaching the wall is totally suppressed in a narrow layer of a retarded liquid.

In the present calculations, at the solid boundaries we take

$$U_i = V_i = 0, \quad i = \overline{2, m}.$$

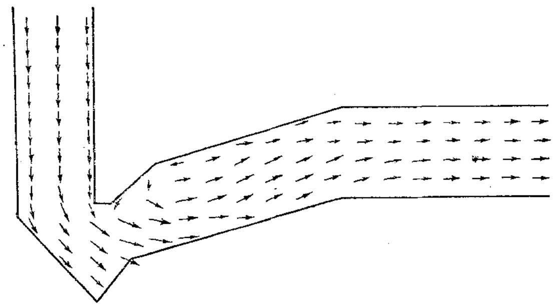

Fig. 3. Averaged velocity field of particles.

An exception is the hopper inclines, where for modeling the particle extraction from the hopper the wall is assumed penetrable for particles, i.e., just as at the outlet boundary, we have:

$$\frac{\partial U_i}{\partial n} = \frac{\partial V_i}{\partial n} = 0, \quad i = \overline{2, m},$$

where n is the coordinate reckoned normally to the surface.

The examined problem was solved numerically on nonuniform staggered grids. The sought values of gas and paticle velocities were determined at the edges of calculating meshes, whereas the values of some parameters were obtained in mesh centers. Discretization of the initial differential equations was carried out by a control volume method [5]. To diminish the effect of numerical diffusion on the final result, oblique differences [6] were employed in approximately the convective terms, which take into account a direction of the flow through the mesh edge. A system of algebraic equations, obtained through approximating the initial differential equations, was solved using the Gauss–Seidel iteration method (for ρ_i, i = 2,..., m and U_i, V_i, i = 1,..., m) and the two-dimensional factorization for the remaining parameters. The SIMPLE algorithm was applied to determine pressure [5]. Convergence of the computational processes was checked by a maximal discrepancy identified for each of the transfer equations, as well as by a flow rate for the carrying and heterogeneous phases and by a pressure correction.

The described mathematical model and computational algorithm were tested for the problem on flow of a monodispersed gas–dust mixture in a tube. Figure 1 gives the results of comparing calculated data with those experimental [7], pertaining to the stabilized flow region. As is clear from the figure, there is a good agreement as to the velocity distributions of the carrying medium and as to the curves of the averaged particle velocities. Furthermore, consideration is given to heat exchange of a uniphase liquid in the tube with a sudden expansion. A satisfactory agreement between the calculated Nusselt numbers behind the stagger and the experimental data [8] is obtained.

Below, some calculated results are presented for the flow of a semidispersed mixture in the turning channel of the gas duct. The gas duct configuration given in Figs. 2-4 corresponds to a real configuration. A triangular stagger at the gas duct bottom is formed by the inclines, along which the particles move to the storing hopper. In computations we isolate three fractions of particles of sizes 50, 100, and 200 μm, with their fractional content comprising 15, 30, and 50%. A mass content of the solid phase in the incoming flow is $\rho_p = 10^{-2}$ kg/m^3. A width of the inlet section equals 0.27 m. A gas and particle velocity at this section inlet is $U_i = 12$ m/sec (i = 1,..., 4). The motion of the heterogeneous mixture is effected in the conditions approaching isothermal.

Figure 2 shows a vector field characterizing the motion of the carrying medium. Evidently, a fairly extended zone of the circulation motion develops behind the flow turning region. In the vicinity of this zone, that is, in the flow core, the gas velocity reaches maximal values. Farther downstream the flow straightens and becomes nearly uniform in the outlet section. Figure 3 gives a vector field of the averaged particle velocities $(\mathbf{W}_p = \sum_{i=2}^{m} \rho_i \mathbf{W}_i / \rho_p)$. At the inlet and outlet sections of the gas duct a coincidence of the gas and particle velocity fields is observed, whereas in the turning zone the mixture motion is of nonequilibrium character. This manifests itself in varying sizes of the circulation region of the particle motion and in an increasing angle, which defines the particle onflow to the lower part of the turning section surface. This zone is the most susceptible to erosion wear. Predictions indicate a noticeable particle accumulation at the lower surface of the gas duct, immediately behind the turning section ($\rho_{p\max} = 0.14$ kg/m^3). The latter is due to a significant sluggishness of the relatively large parti-

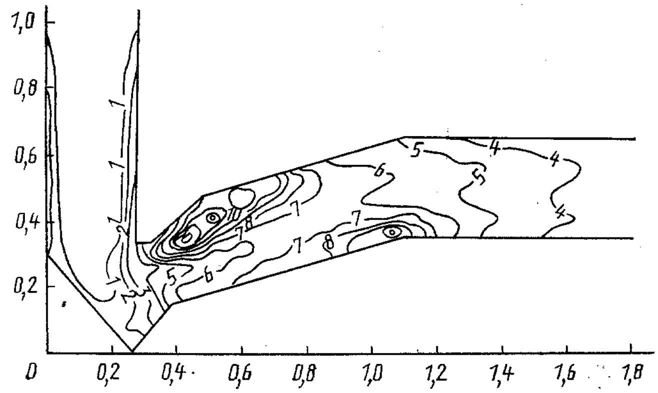

Fig. 4. Isolines of turbulent fluctuation energy.

TABLE 1. Efficiency of the Particle Entrapment in the Hopper

d_p, μm	Q_{inlet}, g/sec	Q_{inlet}, g/sec		
		1	2	3
50	4,9	4,9	4,0	4,9
100	9,3	4,9	5,2	4,9
200	16,8	3,8	6,7	3,7
Total	31	13,6	15,9	13,5

cles (d_p = 100, 200 μm), which are cast onto the channel wall on an abrupt change in the motion direction of the carrying medium.

Figure 4 demonstrates isolines for the kinetic energy of turbulence K (m^2/sec^2). Clearly, in the inlet section, the development of a turbulent structure accompanies the growth of boundary layers, therefore the zones of elevated intensity of the turbulent fluctuations are localized at the gas duct walls. A marked augmentation of the general background in the intensity distribution occurs behind the turning region, which is linked to transition of a certain portion of the kinetic energy of the averaged motion to the fluctuation energy, in consequence of an appreciable variation in the pulse entering the turning flow section. Moreover, there are two regions of elevated turbulent fluctuation intensity on this background. One of them coincides with the circulation motion zone (a large vortex immediately behind the turning section), and the other conforms to the flow turning in entering the last rectilinear section of the gas duct.

Apart from those presented above, calculations were performed for flows in gas ducts of the given configuration with various inclination angles of the outlet branch to the horizontal. In all cases the outlet section has a horizontal orientation. A considerable effect of this parameter on velocity fields is revealed, and a particle distribution in the flow and over the channel walls is identified. Using the available calculated results, sizes of the zones subjected to intense erosion wear can readily be evaluated. As computations show, with decreasing inclination angle β of the outlet branch the separation zone behind the flow turning region elongates, and at $\beta = 0°$ it stretches actually to the outlet section. The particle accumulation region, forming at the lower wall of the gas duct, also enlarges with decreasing inclination angle. However, at small inclination angles β the particle concentration in these regions is appreciably lower. It should be pointed out that in all the examined cases (β = 0, 15, and 45°) an indistinct zone of the dispersed phase accumulation was registered at the upper wall of the outlet section. As for the turbulent structure, a great flow turbulence in the outlet branch of the gas duct was observed in the cases of a large alteration in the total flow pulse (high values of β).

Efficiency of the particle entrapment in the hopper can be estimated from Table 1. Here Q is the mass flow rate of the particles through the cross section of the gas duct. The values β = 15, 0, and 45° pertain to variants 1, 2, and 3. As is seen from the table, the entrapment efficiency for the considered variants is within 50-60%. The angle alteration differently affects the entrapment of particles of various fractions. By the integral exponent, characterizing the particle entrapment for all fractions, the first and third variants are the most favorable.

The presented computations indicate that for the gas ducts where flows can be approximated as two-dimensional, the proposed mathematical model allows a determination, along with a local aerodynamic flow structure, of integral process characteristics important for engineering calculations. To the latter one should primarily refer efficiency of the particle entrapment and pressure losses on the examined section of the gas duct. Besides, based on analyzing the velocity and concentration fields it is not difficult to locate the zones subjected to erosion wear.

NOTATION

x, y, Cartesian coordinates; U, V, components of the velocity vector; α, ρ, P, T, volume fraction, density, pressure, and temperature; F_x, F_y, components of the force of interphase interaction; μ_t, σ_n, turbulent viscosity coefficient and turbulent Prandtl number; R, gas constant; g, acceleration due to gravity; K, kinetic energy of turbulence; ε, dissipation of turbulence energy; δ_{ij}, Kronecker symbols; D, tube diameter; $\rho_i^0 = \rho_i/\alpha_i$, true density; μ_1, λ_1, viscosity and thermal conductivity coefficients of the carrying medium; d_{pi}, dimension of the i-th particle fraction; ρ_p^0, true density of the particles; β, inclination angle of the outlet branch of the gas duct to the horizontal. Subscripts: i = 1, parameters of the carrying medium; i = 2, 3, ... , m fractions of the dispersed medium; m − 1, number of fractions.

LITERATURE CITED

1. R. I. Nigmatulin, Fundamentals of Mechanics of a Heterogeneous Medium [in Russian], Moscow (1978).
2. F. Paurahmadi and I. A. C. Hamphrey, Phys. Chem. Hydrodynamics, **4**, 191-219 (1983).
3. B. E. Launder and D. B. Spalding, Comp. Meth. Appl. Mech. Eng., **3**, 269-289 (1974).
4. R. I. Nigmatulin, Dynamics of Multiphase Media [in Russian], Moscow (1987), Part 1.
5. S. Patankar, Numerical Methods for Solving the Problems of Fluid Heat Exchange and Dynamics [in Russian], Moscow (1987).
6. F. D. Raithby, Comp. Meth. Appl. Mech. Eng., **9**, 153-180 (1976).
7. Kramer and Depew, Teor. Osnovy Inzh. Rasch., **94**, No. 4, 27-35 (1972).
8. Bon, Hoffman, Takahasi, and Launder, Teploperedacha, No. 4, 91-100 (1984).